ADVANCES IN ATMOSPHERIC SCIENCES, VOL. 32, AUGUST 2015, 1063–1076

Relationships among the Monsoon-like Southwest Australian Circulation, the Southern Annular Mode, and Winter Rainfall over Southwest Western Australia

FENG Juan[1,2,3], LI Jianping*[1,3], Yun LI[4], ZHU Jianlei[2], and XIE Fei[1]

[1]*College of Global Change and Earth System Science, Beijing Normal University, Beijing* 100875

[2]*State Key Laboratory of Numerical Modeling for Atmospheric Sciences and Geophysical Fluid Dynamics, Institute of Atmospheric Physics, Chinese Academy of Sciences, Beijing* 100029

[3]*Joint Center for Global Change Studies, Beijing* 1000875

[4]*Data Analytics, CSIRO Digital Productivity FlagshipFloreat,* 6083*, Western Australia, Australia*

(Received 1 July 2014; revised 23 December 2014; accepted 29 December 2014)

ABSTRACT

This study examines the relationships among the monsoon-like southwest Australian circulation (SWAC), the Southern Annular Mode (SAM), and southwest Western Australia winter rainfall (SWR), based on observed rainfall, reanalysis datasets, and the results of numerical modeling. By decomposing the SWAC into two components using a linear model, i.e. the component related to SAM (RSAM) and the component unrelated to SAM (SWACI*), we find it is the SWACI* that shows a significant influence on SWR. Similarly, it is the component of SAM associated with SWAC that exhibits an impact on SWR, whereas the component unrelated to SAM. A similar result is obtained in terms of the circulation associated with SWAC and the SAM. These facts suggest the SAM plays an indirect role in influencing SWR, and raise the possibility that SWAC acts as a bridge between the SAM and SWR, by which the SAM passes its influences onto SWR. This is due to the fact that the variations of SWAC are closely linked to the thermal contrast between land and sea across the southern Indian Ocean and southwest Australia. By contrast, the SAM does not significantly relate to this thermal structure, particularly for the component unrelated to SWAC. The variations of surface sea temperature over the southern Indian Ocean contribute to the favored rainfall circulation patterns. This finding is supported by the numerical modeling results. The strong coupling between SWAC and SWR may be instrumental for understanding the interactions between SWR and the southern Indian Ocean, and provides another perspective in examining the variations in SWR.

Key words: monsoon-like Southwest Australian Circulation, Southern Annular Mode, southwest Western Australian winter rainfall

Citation: Feng, J., J. P. Li, Y. Li, J. L. Zhu, and F. Xie, 2015: Relationships among the monsoon-like southwest Australian circulation, the Southern Annular Mode, and winter rainfall over southwest Western Australia. *Adv. Atmos. Sci.*, **32**(8), 1063–1076, doi: 10.1007/s00376-014-4142-z.

1. Introduction

Southwest Western Australia (SWWA) is located in the southwest corner of the Australian continent (30°–35°S, 115°–120°E). The rainy season is from May to October, corresponding to the austral winter half-year. Since the middle of the 20th century, the observed SWWA winter (June–August, JJA) rainfall (SWR) has decreased by about 15%–20% of the preceding 50-yr average (IOCI, 2002), resulting in an even sharper fall in stream flow in southwestern Australia, which has strongly influenced the availability of water resources in the region.

The recent decrease in rainfall within SWWA has been intensely studied. For instance, previous works have reported that the rainfall reduction is associated with large-scale variations in sea level pressure (SLP; e.g., Allan and Haylock, 1993; Ansell et al., 2000; IOCI, 2002), northwest cloudiness bands (e.g., Telcik and Pattiaratchi, 2014), SST over the Indian Ocean (e.g., Nicholls, 1989; Smith et al., 2000), as well as the shift of storm tracks (e.g., Smith et al., 2000; Frederiksen and Frederiksen, 2007). Other studies have implicated the influences of variations in land surface processes within SWWA (e.g., Lyons, 2002; Pitman et al., 2004; Timbal et al., 2006) or anthropogenic activities (e.g., Hope, 2006; Timbal and Arblaster, 2006). Bates et al. (2008) provided a detailed review of the factors contributing to the decrease in SWR. Recently, Feng et al. (2010a) proposed a monsoon-like south-

* Corresponding author: LI Jianping
Email: ljp@bnu.edu.cn

west Australian circulation (SWAC) over the wider SWWA, which explains either interannual variations in rainfall over SWWA or the long-term drying trend, and the study indicated that the variability in SWAC has contributed to the reduction in SWR.

The prominent mode of climatic variability throughout the Southern Hemisphere is the Southern Annular Mode (SAM; Gong and Wang, 1999; Thompson and Wallace, 2000). This mode is characterized by an approximately zonal symmetry, with pressure anomalies of one sign centered about 40°–50°S and anomalies of the opposite sign centered in the Antarctic. It is reported that this mode has been increasing towards higher polarity since the late 1960s (e.g., Nan and Li, 2003; Marshall, 2003; Visbeck, 2009); and some studies have attributed the decreasing of SWR to the concurrent strengthening of the SAM (e.g., Ansell et al., 2000; Cai and Watterson, 2002; Meneghini et al., 2007). However, Hendon et al. (2007) indicated that there is little evidence that the SAM has contributed to seasonal precipitation change over Australia during the past 25 years (i.e., 1979–2004), except in summer. Focusing on these ambiguities regarding the relationship between the SAM and SWR, Feng et al. (2010b) illustrated that the apparent inverse relationship between the SAM and SWR is caused by an extreme year, 1964. They documented that the SAM shows little influence on SWR in both the periods prior to and after 1964, as determined by analysis that excluded the data for 1964 in the period 1948–2007. These results regarding SAM and SWR were further checked by Cai et al. (2011), who reported that the SAM affects 2–7-day synoptic weather systems over SWWA based on the post-1979 data. To this point, whether the SAM has an influence on the SWR in the seasonal scale remains inconclusive. Our results show that the correlation coefficient between SAM and SWR is -0.41 during 1979–2010, significant at the 0.05 level [same period as in Cai et al. (2011)]; however, the correlation (-0.28) is not significant when the data for 2010 are excluded (i.e., 1979–2009). Importantly, the winter of 2010 corresponds to maximum SAM index (SAMI) values during 1948–2010, and the winter rainfall over SWWA is the lowest, indicating a totally opposite situation to the case in 1964 (Feng et al., 2010b). Also important is that the year 1998 is a large year for SAMI too, but SWR is normal. These findings indicate that the relationship between SWR and the SAM is unstable in the period 1979–2010.

Variations in SWR are strongly coupled with SWAC, which in turn is closely linked to the SAM (Feng et al., 2010a, Fig. 8c), and yet the SAM has little direct influence on SWR. It is therefore interesting to question the relationships among these three phenomena: Does the influence of the SAM on SWAC generate a response in SWR? If so, what is the associated physical process? If not, what is the role of the SAM in influencing SWAC, and why does the SAM have little influence on SWR? Is it due to the external forces of SWAC being independent of the SAM? The above considerations provided the main motivation for the present study. That is, to clarify the relationships among SWAC, the SAM, and SWR, and to explain why the SAM plays a non-significant role in influencing the variations of SWR. It is important that we have some idea of the factors causing the variations in SWR, especially given the recent decline in SWR.

The remainder of the paper is arranged as follows. The datasets, method, and model are described in section 2, and the relationships among SWAC, the SAM, and SWR are analyzed in section 3. Section 4 explains why the SAM plays a non-significant role in influencing SWR, and explores the impacts of SWAC external forces on SWR. Finally, conclusions and further discussion are presented in section 5.

2. Data, method, and model

The datasets used in this study include high-resolution gridded rainfall on a $0.25^\circ \times 0.25^\circ$ horizontal resolution from 1948 to 2010 (Jones and Bead, 1998), provided by the Australian Bureau of Meteorology. The atmospheric fields are from the National Centers for Environmental Prediction/National Center for Atmospheric Research (NCEP/NCAR) reanalysis (Kalnay et al., 1996). The global SST is from the Met Office Hadley Centre's sea ice and SST datasets, gridded at $1^\circ \times 1^\circ$ resolution (Rayner et al., 2003), and the Improved Extended Reconstruction SST (Smith and Reynolds, 2004) with a resolution of $2^\circ \times 2^\circ$. The SAMI is defined as the difference in normalized monthly zonal-mean SLP between 40° and 70°S (Nan and Li, 2003), using the NCEP/NCAR reanalysis. The SAMI used is strongly correlated with the SAM index defined as the leading Empirical Orthogonal Function of SLP anomalies south of 20°S (Thompson and Wallace, 2000), yielding a correlation coefficient of 0.96 during JJA for the period 1948–2007 (Feng et al., 2010b). Thus, the SAMI used is appropriate in terms of capturing the features of the SAM. The SWAC index (SWACI) is defined following Feng et al. (2010a), based on the dynamical normalized seasonality monsoon index introduced by Li and Zeng (2002). This index is based on the intensity of the seasonality of the wind field, and can be used to depict the seasonal cycle and interannual variability of monsoon over different areas. Given a pressure level and a gird point (i, j), the dynamical normalized seasonality index in the mth month of the nth year is given by

$$\delta_{n,m}(i,j) = \frac{\|\boldsymbol{V}_1(i,j) - \boldsymbol{V}_{n,m}(i,j)\|}{\|\boldsymbol{V}(i,j)\|} - 1 \,, \qquad (1)$$

where $\boldsymbol{V}_1(i,j)$ (m s^{-1}) is the January climatology (averaged from 1968 to 1996 as the reference state) wind vector, and $\boldsymbol{V}_{n,m}(i,j)$ (m s^{-1}) represents the wind vectors at grid point (i,j) in the mth month of the nth. $\boldsymbol{V}(i,j)$ (m s^{-1}) represents the mean of January and July climatology wind vectors (averaged from 1968 to 1996) at grid point (i,j). The norm $\|A\|$ is defined as $\|A\| = (\iint |A|^2 dS)^{\frac{1}{2}}$, where S denotes the domain of integration. At a given grid point (i,j),

$$\|A_{i,j}\| \approx \Delta s[(|A^2_{i-1,j}| + 4|A^2_{i,j}| + |A^2_{i+1,j}|)\cos\varphi_j + |A^2_{i,j-1}|\cos\varphi_{j-1} + |A^2_{i,j+1}|\cos\varphi_{j+1}]^{\frac{1}{2}} \,,$$

where φ_j is the latitude at the point (i, j) and $\Delta s = a\Delta\varphi\Delta\lambda/4$, in which a is the mean radius of the Earth, and $\Delta\varphi$ and $\Delta\lambda$ (in radians) are resolutions in the meridional and zonal directions, respectively. Having obtained the dynamical normalized seasonality index $\delta_{n,m}(i, j)$ at a grid point (i, j), the SWACI is defined as the areal mean of $\delta_{n,m}(i, j)$ over the domain (35°–25°S, 100°–145°E) at 850 hPa.

The atmospheric general circulation model employed is the NCAR Community Atmospheric Model, version 3 (CAM3). This model is able to reproduce the climate features as observed (e.g., Li et al., 2012; Feng and Li, 2013), and serves as the atmospheric component of the Community Climate System Model (CCSM). The horizontal resolution is T42 (approximately $2.8° \times 2.8°$), with 26 hybrid vertical levels. A complete description of this model version is available online at http://www.ccsm.ucar.edu/models/atm-cam/docs/description/.

To explore the influence of the SAM on the SWAC response to SWR, a partitioning of the SWACI is derived as follows:

$$\mathrm{SWACI} = \mathrm{RSAM} + \mathrm{SWACI}^* , \tag{2}$$

$$\mathrm{RSAM} = r\frac{\sigma(\mathrm{SWACI})}{\sigma(\mathrm{SAMI})}\mathrm{SAMI} , \tag{3}$$

$$\mathrm{SWACI}^* = \mathrm{SWACI} - r\frac{\sigma(\mathrm{SWACI})}{\sigma(\mathrm{SAMI})}\mathrm{SAMI} , \tag{4}$$

where RSAM is SWAC variability related to the SAM (represented by a linear fit of SAMI to SWACI), with SWACI* being the component of SWAC that is unrelated to the SAM; r denotes the correlation coefficient between SWACI and SAMI; and σ (SWACI) and σ (SAMI) are the standard deviations of SWACI and SAMI, respectively. Then, the corresponding explained variance fraction of RSAM(RS) and SWACI* (RG) to SWAC is obtained as follows:

$$S^2_{\mathrm{RSAM}} = \frac{1}{n}\sum(\mathrm{RSAM} - \overline{\mathrm{SWACI}})^2 , \tag{5}$$

$$S^2_{\mathrm{SWACI}^*} = \frac{1}{n}\sum(\mathrm{SWACI} - \mathrm{RSAM})^2 , \tag{6}$$

$$S^2_{\mathrm{SWACI}} = \frac{1}{n}\sum(\mathrm{SWACI} - \overline{\mathrm{SWACI}})^2 , \tag{7}$$

$$\mathrm{RS} = \frac{S^2_{\mathrm{RSAM}}}{S^2_{\mathrm{SWACI}}} , \tag{8}$$

$$\mathrm{RG} = \frac{S^2_{\mathrm{SWACI}^*}}{S^2_{\mathrm{SWACI}}} , \tag{9}$$

where $\overline{\mathrm{SWACI}}$ is the mean value of SWACI. Accordingly, the sum of RS and RG is equal to 1. Using this method, SWAC can be separated into two components, i.e., RSAM and SWACI*. The component RSAM is related to SAM, reflecting the variations in SWAC associated with SAM. The other component, SWACI*, is the component of SWAC that is linearly independent of the SAM. Similarly, a partitioning of the SAMI is derived as follows:

$$\mathrm{SAMI} = \mathrm{RSWAC} + \mathrm{SAMI}^* , \tag{10}$$

where the RSWAC indicates the component of the SAM related to SWAC, reflecting the variations in the SAM associated with SWAC; and the SAMI* is the component of the SAM that is linearly independent of SWAC. Consequently, we are able to assess whether the influence of SWAC on SWR is a reflection of the SAM. Here, the austral winter season (JJA) is the focus, which corresponds to the SWWA rainy season and demonstrates significant long-term rainfall trends. Moreover, given that both SWR and the SAM show significant linear trends, the detrended data are used to examine the relationships among SWAC, the SAM, and SWR, to better indicate the nature of the relationships on interannual timescales (Li et al., 2005), unless otherwise stated. The study period spans from 1948 to 2010. We have established that relationship between SWAC and SWR is robust for the whole study period, and have demonstrated that their relationship is reliable when the data before 1979 are employed (Feng et al., 2010a, 2010b).

3. Relationships among SWAC, the SAM, and SWR

To assess whether the relationships are robust between SWAC and the SAM, and between SWAC and SWR, the correlations among them (excluding the extreme year of 1964) are further checked according to Feng et al. (2010b). We find that the relationships between the SWACI and SWR are robust with a correlation coefficient of 0.74, yielding a correlation coefficient of 0.67 when the data for 1964 are excluded. This suggests that the SWAC–SWR relationship is coherent. Similarly, a significant relationship is observed between SWAC and the SAM, with a correlation coefficient of -0.50 when the 1964 data are included, and -0.42 when they are excluded, both exceeding the 0.05 level of significance. These results suggest stable relationships between SWAC and the SAM, and between SWAC and SWR; i.e., a strong SAM is associated with weak SWAC, and weak SWAC is associated with reduced SWR. However, the SAM has a non-significant influence on SWR when the data for 1964 are excluded (Feng et al., 2010b, Fig. 1c and Table 1), raising the question of whether it is possible that SWAC is a bridging medium between the SAM and SWR, i.e., the SAM first plays a role in influencing the variations of SWAC, which in turn affects SWR. That is, the SAM plays an indirect role in influencing SWR. To explore this possibility, the variability of SWAC/SAM is divided into two irrespective components by employing the method described in section 2. Figure 1 shows the correlation maps between Australian winter rainfall and the time series of SWACI, SWACI* and RSAM, as well as those of SAMI, SAMI* and RSWAC. Note that the correlations of RSAM/SWACI* and RSWAC/SAMI* are multiplied by their corresponding explained variance fraction of SWACI and SAMI, so that their sum is equal to the raw correlation between SWACI/SAMI and precipitation. The combined influence of RSAM and SWACI* on SWR mainly reflects the role of SWACI*, since RSAM only accounts for 29% of the explained variance of SWAC, whereas SWACI* accounts for

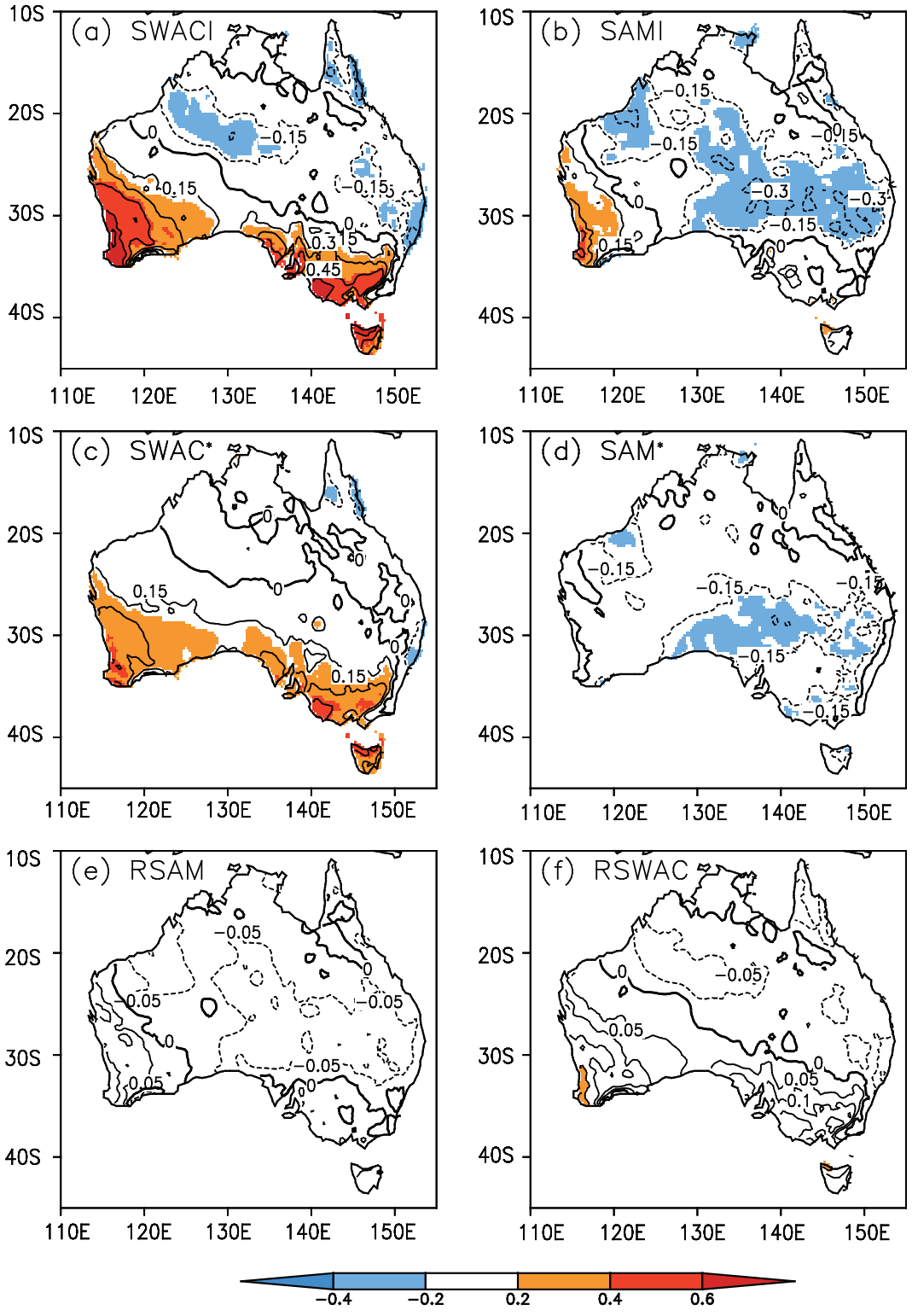

Fig. 1. Left panels: detrended correlation maps between Australian winter rainfall and (a) SWACI, (c) the fraction of SWACI unrelated to SAM (SWACI*), and (e) the fraction of SWACI related to SAM (RSAM). The values in (c) and (e) are multiplied by the fraction of SWACI variance explained by SWACI* and RSAM, respectively, so that their sum is equal to the values in (a). Right panels: as in the left panels, but for the result of SAMI; the sign of the relation is reversed to enable a direct comparison with SWAC.

71%. This result indicates that the influence of SWAC on SWR is largely independent of fluctuations in the SAM, although SAMI and SWACI are moderately correlated (correlation coefficient of −0.50). By contrast, the combined in-

Table 1. The combinations of SWAC and the SAM divided by their corresponding index values. The positive, neutral and negative polarities correspond to the values above, within and below one positive, one negative to positive, and one negative standard deviation for the corresponding indices, respectively.

		SAM		
		positive	neutral	negative
SWAC	positive	0	6 (1974, 1981, 1991, 1992, 1996, 2009)	2 (1963, 1964)
	neutral	4 (1979, 1983, 1998, 2004)	33 (1949, 1952, 1953, 1955, 1956, 1958, 1960, 1961, 1962, 1965, 1966, 1967, 1968, 1970, 1971, 1973, 1975, 1977, 1978, 1980, 1982, 1984, 1985, 1986, 1988, 1990, 1994, 1995, 2000, 2002, 2003, 2005)	7 (1948, 1950, 1951, 1954, 1957, 1959, 1972)
	negative	4 (1989, 1993, 2008, 2010)	7 (1969, 1976, 1987, 1997, 1999, 2001, 2006)	0

fluence of RSWAC and SAMI* on SWR is mainly exhibited in the component of RSWAC. This can also be seen from the correlation coefficients among them, i.e., the correlation coefficient between SWACI* and SWR is 0.63, whereas it is only 0.01 between SAMI* and SWR. This further suggests that the variability of the SAM that is unrelated to SWAC (i.e., SAMI*) alone does not have an influence on SWR, although this component takes up the dominant variability (explained variance: $\sim$ 71%) of the SAM.

Next, we consider the relative contributions of SWACI* and RSAM to the anomalous circulation pattern associated with SWAC, and also for those of the SAM. Figure 2 shows the correlation maps between SLP and each of SWACI, SWACI* and RSAM, as well as the maps between SLP and each of SAMI, SAMI* and RSWAC. We can see that SWACI is significantly negatively correlated with SLP in the mid latitudes centered within 90°–150°E, suggesting cyclonic circulation anomalies over the wider SWWA. In addition, conspic-

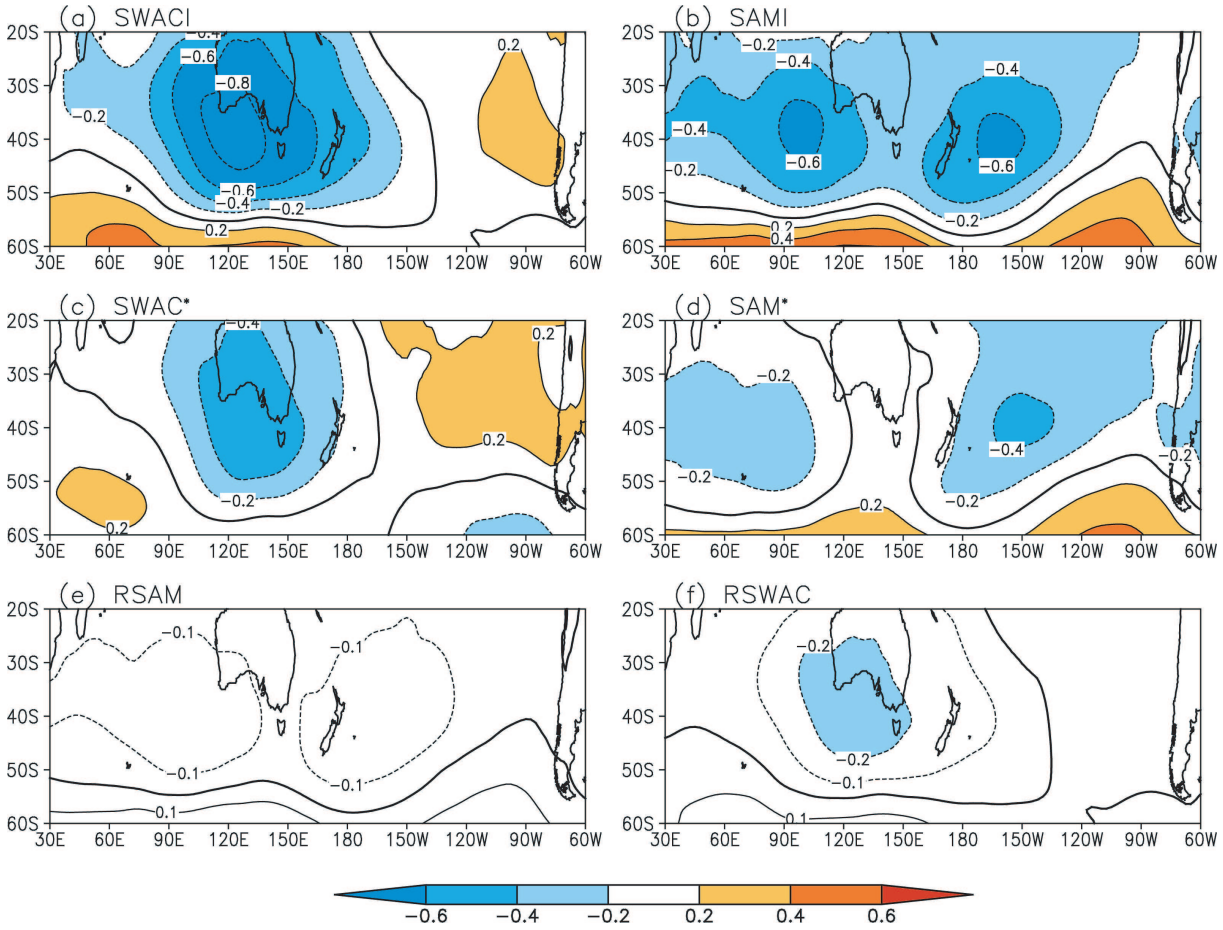

Fig. 2. As in Fig. 1, but for detrended correlations with sea level pressure.

uous positive correlations are seen at high latitudes, corresponding to a subdued zonal gradient, associated with a negative SAM phase (Fig. 2a). For SAMI, an almost opposite situation is observed. Note that the signal of the anomalies associated with SWACI is more regional and less zonal than those related to SAMI. This result that SWAC represents a favorable circulation pattern for rainfall is consistent with the above analyses and with the findings of previous studies (e.g., Cai and Watterson, 2002; Feng et al., 2010a).

Figures 2c and e show the relative contributions of SWACI* and RSAM to the anomalous circulation pattern associated with SWAC. Consistent with the result regarding rainfall, anomalous circulation patterns associated with RSAM are not significant either in the middle or high latitudes; however, significant signals are seen over the wider SWWA for SWACI*, suggesting that this factor makes a dominant contribution to circulation variations associated with SWAC. This result indicates that variations of SWACI* make the dominant contribution to circulation patterns related to SWAC. On the other hand, the significant circulation anomalies linked to SAMI over SWWA is mainly reflected in the component of SAMI which is related to SWACI (Fig. 2f vs 2d), i.e. RSWAC, rather than the component of SAMI*.

The above analyses demonstrate that the component of SWAC that plays a role in influencing SWR (i.e. SWACI*) is largely independent of the SAM, and that the component of SWAC related to SAM (i.e. RSAM) contributes little to variations in SWR. In contrast, the component of the SAM that plays a role in influencing SWR is linked to variations of SWAC (i.e. RSWAC), despite its minor explained variance of the SAM. These results reveal that the relationship between SWAC and SWR is largely due to SWACI*, which is independent of the SAM. However, the relationship between the SAM and SWR is dependent on the component of RSWAC, which is linked to SWAC. That is, SWAC acts as a bridge between the SAM and SWR, by which the influence of the SAM can pass onto SWR, i.e. the SAM plays an indirect role in influencing SWR.

To further establish the above conclusion about the influence of SWAC and the SAM on SWR, the SWAC and SAM are divided into three polarities (positive, neutral, and negative), commonly utilized in analyzing ENSO events, in which positive polarities correspond to values above one standard deviation, neutral polarities corresponds to values within one negative to positive standard deviation, and negative polarities for the events below one negative in the corresponding indices, respectively. Accordingly, there are nine combinations, as listed in Table 1. We see that no case exists for the combinations of positive SWAC–positive SAM, or negative SWAC–negative SAM during the period 1948–2010. The combination that occurs most frequently is neutral SWAC–neutral SAM, with a frequency of 33 years. The corresponding anomalous rainfall patterns associated with these combinations are shown in Fig. 3. Since there are no cases of positive SWAC–positive SAM or negative SWAC–negative SAM, the corresponding figures are blank in Figs. 3a and i, and Figs. 4a and i. We can see abundant rainfall during positive SWAC years, regardless of the SAM year over SWWA being neutral or negative. Negative rainfall anomalies are apparent during negative SWAC years in both positive and neutral SAM years. This point shows that positive/negative SWAC years are associated with more/less SWR, regardless of the SAM's polarity. However, during positive SAM years, rainfall anomalies in neutral and negative SWAC years are different, i.e. with positive values during neutral SWAC years but negative anomalies in negative SWAC years. In particular, positive rainfall anomalies are observed during positive SAM–neutral SWAC, which cannot be explained by the notion that SAMI is negatively correlated with SWR, as reported in previous studies (e.g., Cai et al., 2005). Furthermore, the rainfall anomalies during negative SAM years are also inconsistent in the combinations with positive or neutral SWAC years. Note that there are basically negative rainfall anomalies during negative SAM–neutral SWAC, which conflicts with previous studies (e.g., Cai et al., 2005). This in turn supports the result that the role of the SAM in impacting SWR occurs via SWAC. Note that during neutral SWAC years, the anomalous percentage of SWR is within 20%, between the positive and negative SAM years, but it is beyond 40% from the positive to negative SWAC years, even with the combination of neutral SAM years. Moreover, when the events of SWAC and the SAM simultaneously occur, [e.g. during positive SWAC–negative SAM, and negative SWAC–positive SAM (Figs. 3b and h vs Figs. 3c and g)], the rainfall anomalies are larger than those when the SWAC alone occurs, indicating the SAM plays a role in influencing SWAC, and in turn SWR. The above discussion further indicates that the variations of SWR are mainly attributable to the variations of SWAC, and the SAM plays an indirect role in influencing SWR.

The corresponding circulation patterns in these combinations are illustrated in Fig. 4. The circulation patterns favoring more SWWA rainfall are observed in positive SWAC years for the combinations either in neutral (Fig. 4b) or negative (Fig. 4c) SAM years, i.e. strengthened westerlies and negative geopotential height anomalies over SWWA (e.g., Smith et al., 2000). Accordingly, circulations suppressing SWR are observed during negative SWAC years in the combinations both with positive (Fig. 4g) and neutral (Fig. 4h) SAM years. Moreover, the circulations anomalies over SWWA are opposite in neutral SAM years, with the combinations of positive (Fig. 4b) and negative (Fig. 4h) SWAC years, which is consistent with the rainfall anomalies shown in Fig. 3. This result supports the conclusion that the circulation anomalies associated with SWAC are not the response of the SAM. In particular, no significant signal can be seen either in geopotential height or low-level troposphere winds in neutral SWAC years over SWWA, regardless of the polarity of the SAM (Figs. 4d–f). The result here is consistent with the anomalous rainfall distribution shown in Fig. 3, and further demonstrates that the variations of the SAM act indirectly in impacting SWR. Note that the circulation anomalies associated with SWAC present as a more regional signal than those with the SAM (Figs. 4b and h vs Figs. 4d and f), which

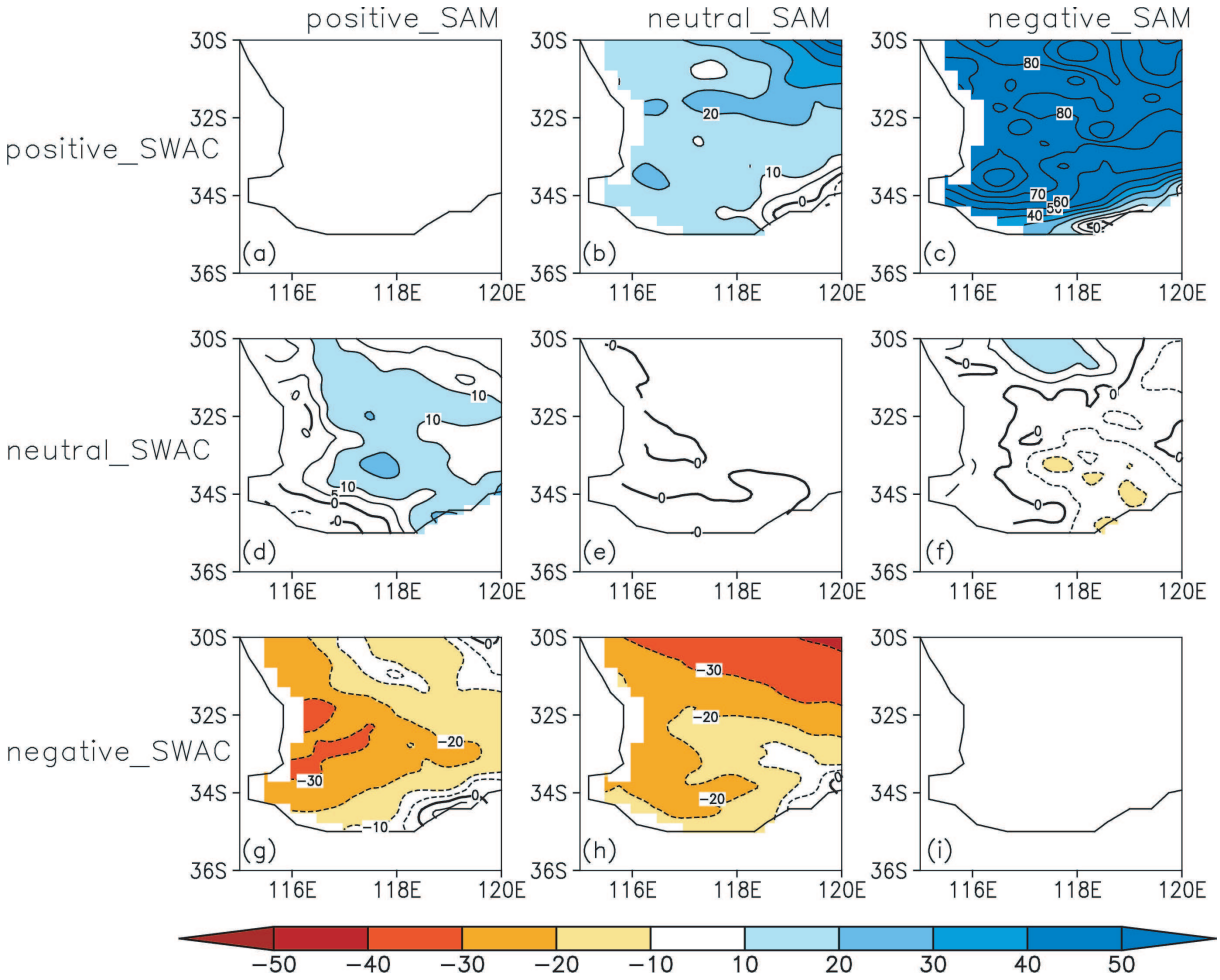

Fig. 3. The anomalous rainfall percentage relative to the climatological mean in the combinations of (a) positive SWAC–positive SAM, (b) positive SWAC–neutral SAM, and (c) positive SWAC–negative SAM. Panels (d–f) and (g–i) are as in (a–c), but for the combinations with neutral and negative SWAC years, respectively (units: %).

is different to previous studies' findings about the zonal-wave pattern (wavenumber 3) associated with SWR (e.g., Allan and Haylock, 1993). On the other hand, it seems that when SWAC and SAM events occur simultaneously (Figs. 4c and g), the center of anomalous circulation shows a westward shift compared to years when SWAC alone occurs (Figs. 4c and g vs Figs. 4b and h), consistent with the SWR anomalies. This raises the possibility that the variations of SWAC are to some extent linked to the longwave trough, which would strengthen the anomalous circulation over SWWA.

4. External drivers of SWAC

The above results suggest that variations in SWAC related to SWR are not influenced by the SAM, possibly because the external factors that drive variations in SWAC are independent of the SAM. Accordingly, this section examines the external forces that drive SWAC. Previous studies have already indicated that the variations of SST across the Indian Ocean appear to contribute to variations of SWR (e.g., Nicholls, 1989; Smith et al., 2000; England et al., 2006). And the variation of land–sea thermal contrast is known to be an important driver of monsoon circulation (e.g., Ramage, 1978; Tao and Chen, 1987; Zhu et al., 1992). Therefore, we analyze the contributions of underlying thermal anomalies to the variations of SWAC.

Figure 5 shows the spatial pattern of the correlation between SWACI/SAMI and SST (over sea)/skin air temperature (SAT, over land), as well as with SWACI*/SAMI*. Significant negative correlations between SWACI and SST are observed west of SWWA, over the southern Indian Ocean, while significant positive correlations are seen over inland areas of southwest Australia. One thing to note is the location of the SST anomalies here is eastward compared to the P2 box in England et al. (2006), in which the role was emphasized of the SST gradient within the Indian Ocean on SWR. The location is also dissimilar to that in Allan and Haylock (1993), which paid attention to the tropical SST in the Indian Ocean. Besides, positive SST anomalies are seen at high latitudes (50°–60°S) within 100°–140°E both for those with SWACI and SWACI*. The distribution of anomalous SAT–SST indicates that the land–sea thermal contrast within

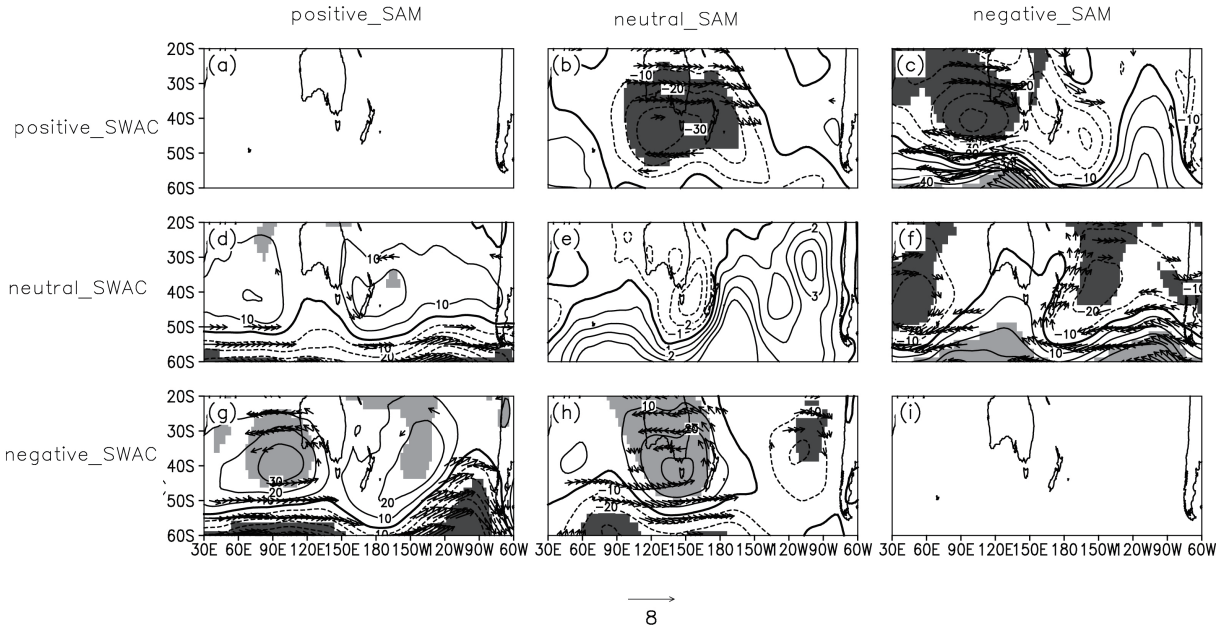

Fig. 4. As in Fig. 3, but for the distributions of anomalous geopotential height (contours; units: gpm) and winds (vectors; units: m s^{-1}) at 850 hPa. Shading indicates statistical significance at the 0.05 level for geopotential height; only wind values significant at the 0.05 level are shown.

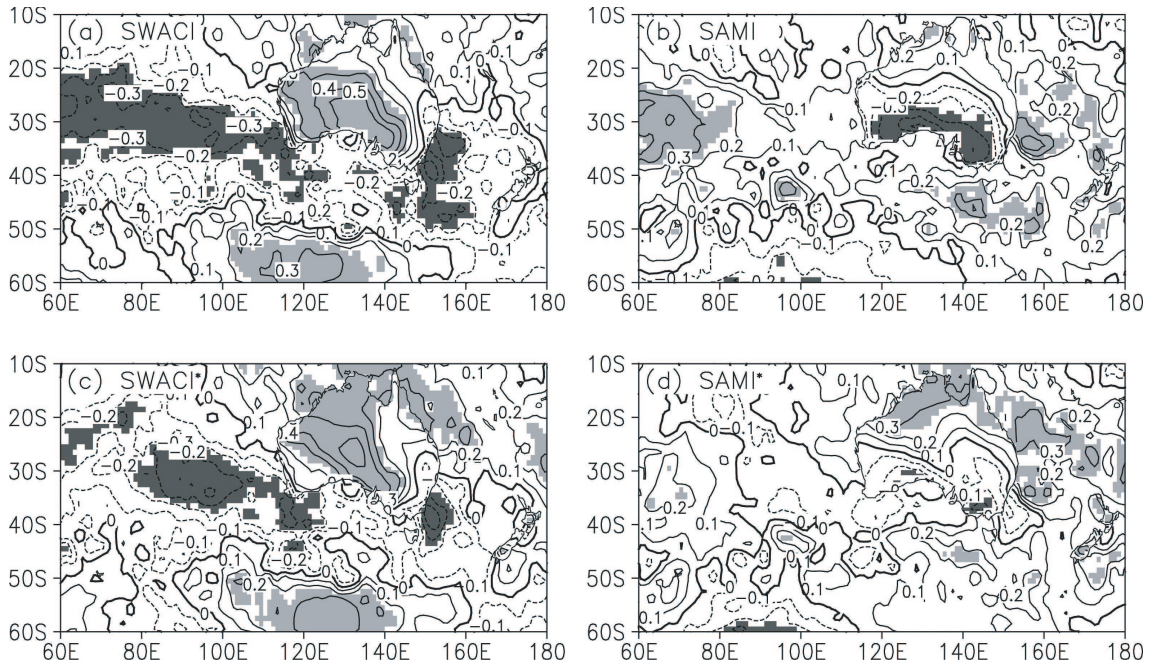

Fig. 5. Detrended correlations between (a) SWACI and SST (over sea) and skin air temperature (over land). (b) As in (a), but for SAMI. (c) As in (a), but for the component of SWACI*. (d) As in (a), but for the component of SAMI*. Shading indicates statistical significance at the 0.05 level.

the southern Indian Ocean and south Australia (35°–25°S, 80°–145°E; LSTC) is intensified in positive SWAC years, in turn implying that the strength of SWAC is closely related to LSTC (SAT minus SST; Fig. 6); this relationship yields a detrended correlation coefficient of 0.57. And the detrended relationship between the SWACI and SST/SAT within (35°–25°S, 80°–145°E) is −0.40/0.48, both significant at the 0.01 level. Accordingly, the relationship between SWR and the SST/SAT within (35°–25°S, 80°–145°E) is −0.47/0.60, implying the variation of SWR is linked to that of SST over the southern Indian Ocean. Most of the features regarding SWAC and the underlying thermal distribution are captured

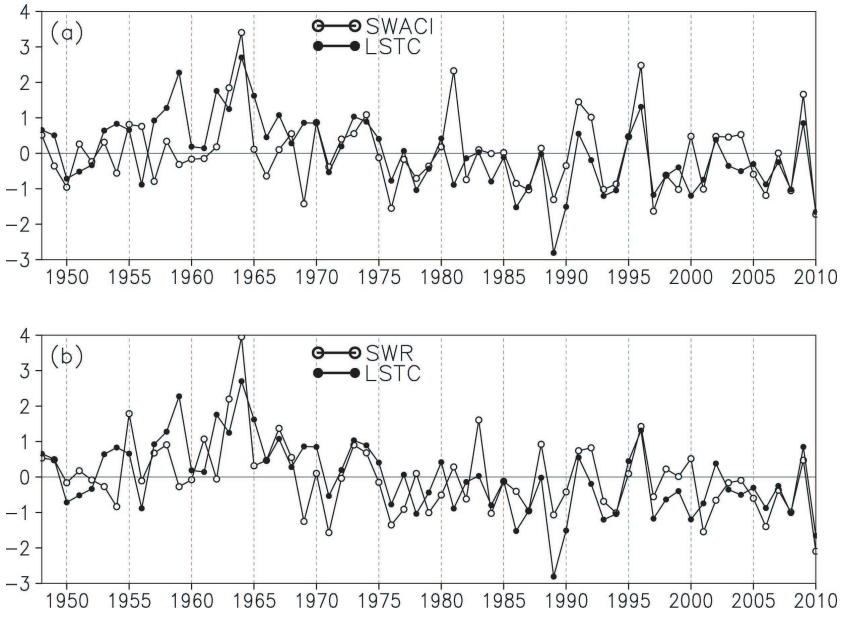

Fig. 6. Normalized time series of SWACI, SWR and land–sea thermal contrast (LSTC) within the region (35°–25°S, 80°–145°E).

by the component of SWAC that is unrelated to the SAM (i.e. SWACI*; Fig. 5c vs Fig. 5a), suggesting this thermal distribution is independent of the SAM.

However, there is an almost non-significant signal in the correlations between SAMI and SST over the southern Indian Ocean, and the correlation coefficient between SAMI and SST within the southern Indian Ocean (35°–25°S, 80°–145°E) is 0.21, suggesting the SAM is not related to the variations of SST within the southern Indian Ocean. Moreover, only a small area along the south coast of Australia shows a significant correlation between the SAMI and SAT (Fig. 5b), consistent with the result in Hendon et al. (2007), yet the signals almost disappear when the effects of SWAC on the SAM are not considered (Fig. 5d). This finding explains why the variability in the SAM plays an indirect role in influencing SWR, for which there is little connection with the variations of SST within the southern Indian Ocean. And the influence of the SAM on SAT over southwest Australia is realized by the component of the SAM related to SWAC (i.e., RSWAC). In contrast, the variation in SST over the southern Indian Ocean is closely associated with the variation in SWAC. These characteristics regarding SST anomalies are consistent with those based on Improved Extended Reconstruction SST data, implying the result is reliable.

To gain insight into the variations in SWAC associated with LSTC, we investigate the temporal changes in tropospheric flow over SWWA by analyzing composite maps of large-scale moist static stability, circulation anomalies, air temperature, vertical velocity, geopotential height, and zonal wind for strong-minus-weak LSTC years (Figs. 7 and 8).

There are clear differences between strong and weak LSTC years in terms of climatic factors. During strong LSTC years, negative SST anomalies occur over the southern Indian Ocean west of SWWA, and positive SAT anomalies occur over southern Australia. Consequently, positive anomalies in air temperature are seen over land and negative anomalies over the ocean (Fig. 7a). Associated with the temperature anomalies, the westerlies over midlatitude regions (20°–40°S) are significantly strengthened throughout the lower and middle troposphere (Fig. 7d), accompanied by negative geopotential height (Fig. 7c); however, high latitudes are marked by positive geopotential anomalies and anomalous easterlies. Strong westerly anomalies occur over the SWAC region, and positive anomalies in moist static stability are observed over the southern Indian Ocean (Fig. 8a), defined by the vertical difference between 300 and 925 hPa pseudoequivalent potential temperature (θ_{se}); consequently, the rising flow over the southern Indian Ocean is suppressed and anomalous subsidence is induced (Fig. 7b). Moreover, the positive SSTA at high latitudes (50°–60°S) within 100°–140°E are associated with SWACI (Figs. 5a and c), implying the easterlies are strengthened within this region. That is, the meridional shear of zonal wind is enhanced, corresponding to a cyclonic anomaly circulation pattern over the region (Fig. 8b). Therefore, the strengthened LSTC acts to strengthen the anomalous subsidence and weaken the atmospheric instability over the southern Indian Ocean, as well as to intensify westerlies in the lower troposphere and ascending flow over southwest Australia. In turn, these changes result in strong SWAC, favoring enhanced winter rainfall over SWWA. The opposite combination of factors is observed during weak LSTC years.

To further verify the above result regarding how LSTC over the southern Indian Ocean and southwest Australia (35°–25°S, 80°–145°E) influences the strength of SWAC, we performed sensitivity experiments with CAM3. The con-

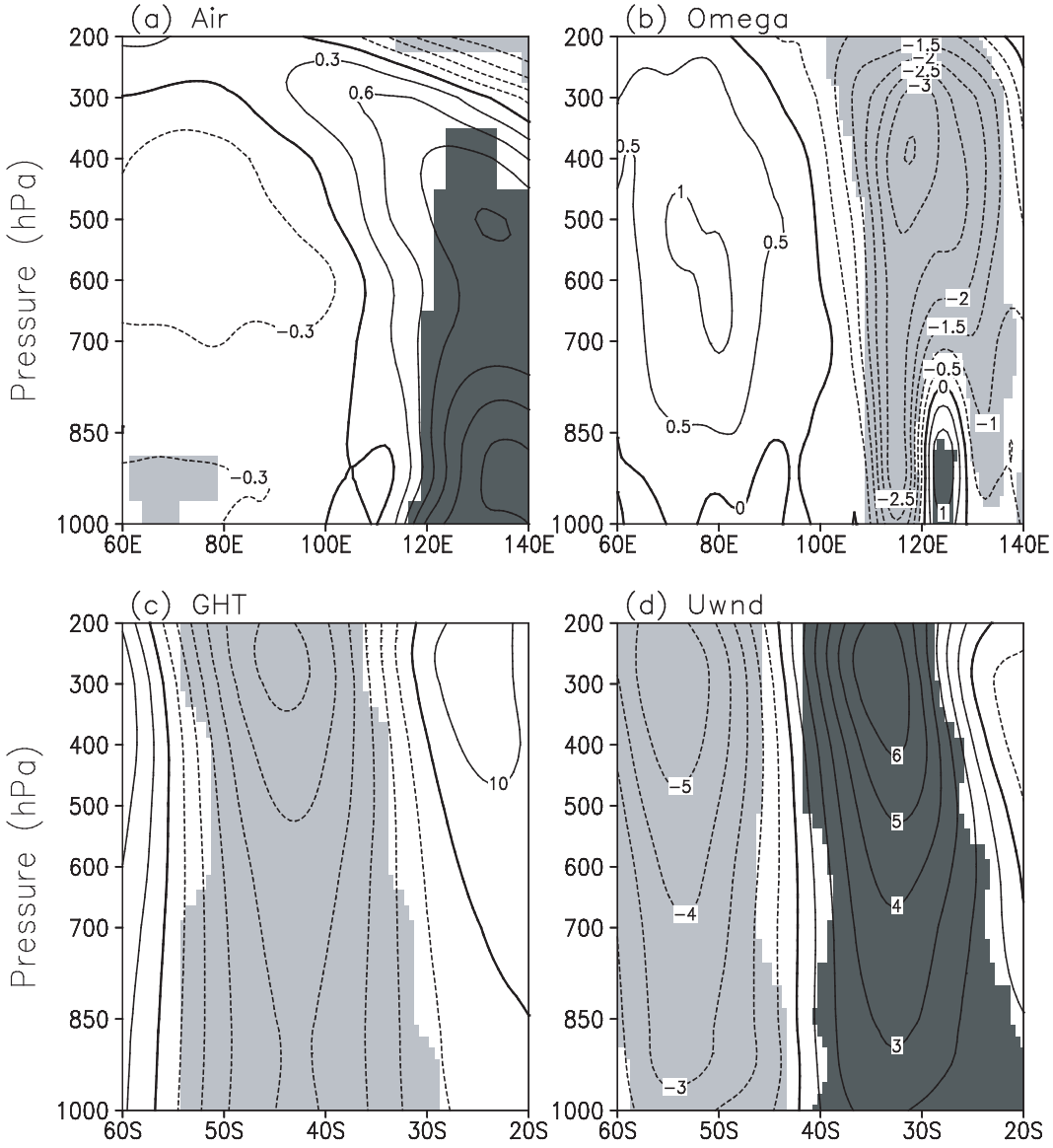

Fig. 7. (a) Longitude–height distribution of composite differences in air temperature between years with strong (greater than +1 standard deviation) and weak (less than −1 standard deviation) LSTC years along 30°S (units: °C). (b) As in (a), but for vertical velocity (ω; units: P s^{-1}). (c) As in (a), but for the latitude–height distribution of composite differences in geopotential height along 115°E (units: gpm). (d) As in (c), but for zonal wind (units: m s^{-1}). Shading indicates statistical significance at the 0.05 level.

trol run was integrated for 25 years to derive a reference state (Fig. 9). Compared with observed circulation patterns, CAM3 performs well in reproducing seasonal features; i.e., the seasonal shift in the subtropical high ridge, being southward in January (Fig. 9c) and northward in July, and the seasonal reversal in the surface prevailing winds over SWWA, being southeasterly in January and northwesterly in July (Fig. 9d). These results provide confidence in the simulation capability of CAM3.

The sensitivity experiments were integrated for 25 years. The integration was used to construct a 25-member ensemble mean, to reduce uncertainties arising from varying initial conditions. Two sets of sensitivity experiments were designed to examine the effects of SST on SWAC over the southern Indian Ocean: one with decreased SST over the region (35°–25°S, 80°–145°E) for ocean areas, and another with increased SST. To mimic and isolate the influences of SST variation, the only difference between the sensitivity and control experiments was a 1°C change in the sensitivity run. Note that the amplitude of the SST anomalies center over the southern Indian Ocean within the strong and weak LSTC years is beyond 0.8°C; that is, the SST adjustment in the sensitivity experiment is comparable to those in the anomalous LSTC years.

Figure 10 displays the difference between the two sets of sensitivity experiments (decreasing SST minus increasing

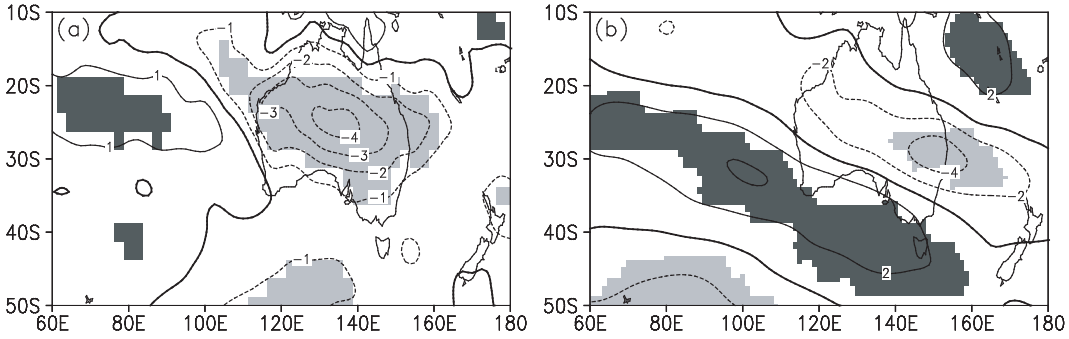

Fig. 8. As in Fig. 7, but for (a) the vertical difference between the 300 and 925 hPa pseudoequivalent potential temperature (θ_{se}) (units: K) and (b) sea level pressure (contours; units: Pa) and wind (vectors; units: m s^{-1}) at 850 hPa.

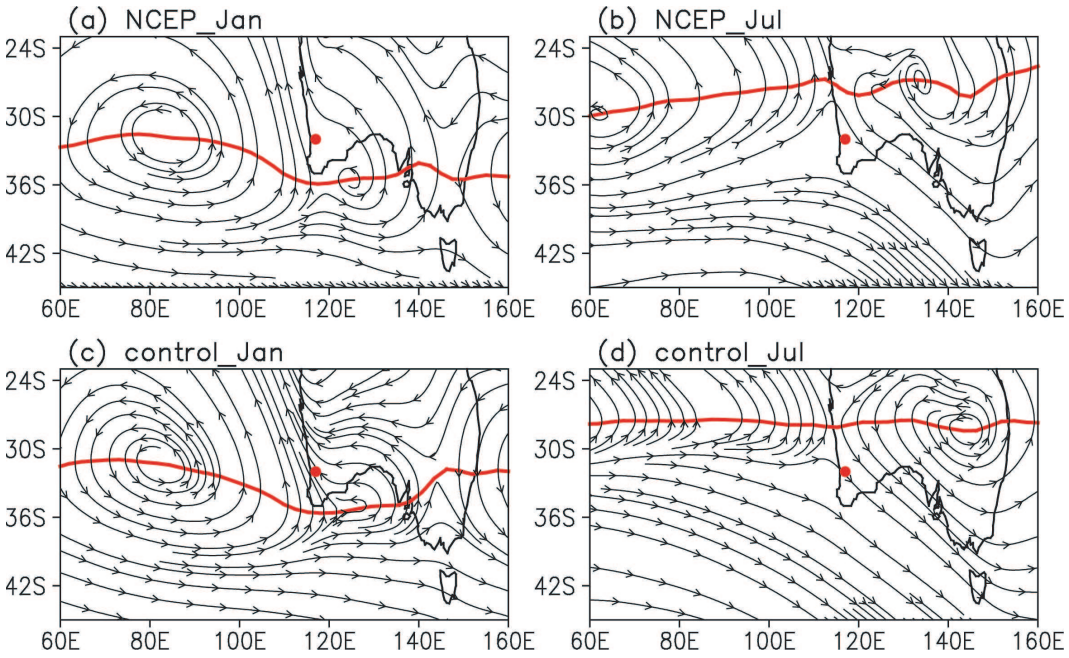

Fig. 9. Averaged streamlines for (a, b) observations and (c, d) the control run of CAM3. Left panels: January; right panels: July. The red line is the ridge of the subtropical high. The red dot indicates the location of Perth, Western Australia.

SST). Since the cold SST anomalies within (35°–25°S, 80°–145°E) induce greater land–sea thermal contrast, the prevailing westerlies are strengthened and negative geopotential height anomalies are excited over SWWA, which would lead to strong SWAC and in turn favor enhanced winter rainfall over SWWA. This point further supports the result based on the reanalysis above, suggesting that SST variations over the southern Indian Ocean contribute to variability in SWAC.

5. Discussions and Conclusions

The continuous decrease in winter rainfall observed over SWWA has attracted much attention in recent years, and the newly reported monsoon-like SWAC shows a well-coupled relationship with SWR, which explains not only the interannual variability in SWR, but also its long-term decreasing trend. Given that the SAM is the dominant mode in the extratropical Southern Hemisphere, its influence on regional climate has been discussed in many studies. The present study investigated the relationships among SWAC, the SAM, and SWR. The results reveal that the component of SWAC that contributes to SWR variation is unrelated to the SAM (i.e. SWACI*), which explains more than 70% of the variance in SWAC. By contrast, the component of the SAM that contributes to variations of SWR is the one related to SWAC (i.e. RSWAC), implying the SAM plays an indirect role in influencing SWR. That is, the effects of the SAM should be via SWAC, and thus contributing to the variability of SWR. This finding reflects the fact that the external drivers of SWAC are largely independent of the SAM. The present analysis reveals that variations in large-scale LSTC within the southern Indian Ocean and southwest Australia contribute to the variability

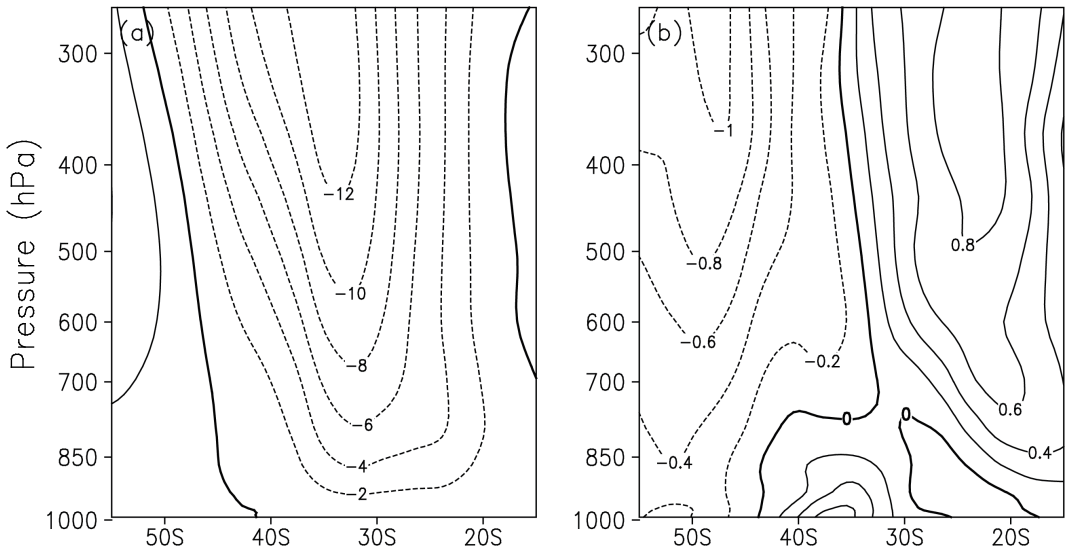

Fig. 10. The anomaly circulation patterns of decreased-minus-increased SST in the sensitivity forcing experiments within the southern Indian Ocean (35°–25°S, 80°–145°E) for the latitude–height cross section of (a) geopotential height (units: gpm) and (b) zonal wind (units: m s^{-1}) along 115°E.

in SWAC. Variations in SST over the southern Indian Ocean have a close link with SWAC, while those of the SAM do not. This explains why the SAM plays a non-significant role in terms of influencing SWR. However, the possible driver of the SST variability over the southern Indian Ocean, not considered in the current study, is an interesting issue worthy of further research.

Furthermore, the winter of 2010 was further examined, taking into account the results from a recent study by Cai et al. (2011) in which it was indicated, based on post-1979 data, that the SAM affects synoptic weather systems over SWWA. The circulation anomalies in the winter of 2010 exhibit positive SAM polarity features (figure not shown). We employed spatial correlation to check the contribution of this circulation pattern to SWR. The spatial circulation pattern of 2010 is marked as P_{2010}, and the correlation patterns between SLP and the RSAM, SWACI*, RSWAC and SAMI* are marked as P_{RSAM}, P_{SWACI*}, P_{RSWAC}, and P_{SAMI*}, respectively. We find that the spatial correlation coefficients between P_{2010} and P_{RSAM}, P_{SWACI*}, P_{RSWAC}, P_{SAMI*}, within (60°–20°S, 30°E–60°W), are −0.85, 0.08, 0.33 and 0.83, respectively. This suggests that P_{2010} shows more similarities to P_{RSAM} and P_{SAMI*}, yet neither P_{RSAM} nor P_{SAMI*} contribute to the variation of SWR (Fig. 2). By contrast, we see that during 1948–2010 SWACI reaches its lowest values in the winter of 2010 (Fig. 6), which corresponds nicely to the variations of SWR. This result implies that the SAM is not responsible for the low winter rainfall in 2010 over SWWA.

Independent of this study, previous studies on the variations of SWR indicate that a shift of the storm track is a contributor (e.g., Smith et al., 2000). Thus, it is worth investigating the potential linkage between the storm track and SWAC. In exploring the linkages between the longwave trough or zonal wavenumber 3 pattern and SWAC, we found that the relationship between SWAC and zonal wavenumber 3 is not significant, with a correlation coefficient of −0.06. This implies that the variation of SWAC is independent from that of zonal wavenumber 3. However, whether or not there are any indirect influences of zonal wavenumber 3 on SWAC, and whether or not the longwave trough plays an impacting role on SWAC, are issues yet to be settled and worthy of further work. In addition, the Antarctic Circumpolar Wave is thought to impact upon southern Australian rainfall (White, 2000). However, it has been reported that the Antarctic Circumpolar Wave could only be seen from 1985 to 1994 (Connolley, 2002), and thus it possibly does not account for the decline in SWR, but could play a role in southern Australian interannual rainfall variability (Meneghini et al., 2007), and perhaps also in SWAC. Therefore, to what degree the Antarctic Circumpolar Wave influences SWAC, as well as the potential linkage and underlying physical mechanism, are open issues that require further work.

Finally, SWAC is a recently reported monsoon-like circulation located in the subtropics, with a seasonal march closely related to the location of the subtropical high within the SWWA region (Feng et al., 2010a). These features are similar to the classical subtropical monsoon system (East Asian summer monsoon, EASM), for which the western Pacific subtropical high (WPSH) has been identified as an important component (e.g., Lau and Li, 1984; Tao and Chen, 1987; Ding, 1994). In addition, the seasonal evolution of the EASM is nicely linked to the northward jump of the WPSH (e.g., Tao and Xu, 1962; Chang et al., 2000; Ding and Chan, 2005). Thus, in what way are the two subtropical monsoon systems similar or dissimilar? Given that both SWAC and the EASM (e.g., Hu, 1997; Li and Zeng, 2002; Guo et al., 2003; Wang and Ding, 2006) have shown a weakening trend in recent decades, it is important to investigate the mechanism un-

derpinning the weakening of these subtropical monsoon systems. Are they being driven by same factors? Are there any factors that may predict the behavior of SWAC? Answers to these questions would have important applications, as variations in SWR could then be predicted, given the relationship between SWAC and SWR. These topics are beyond the scope of the present study but are worthy of further analysis.

Acknowledgements. This work was jointly supported by the 973 Program (Grant No. 2013CB430203), the National Natural Science Foundation of China (Grant Nos. 41205046 and 41475076), and the Australia–China Bilateral Climate Change Partnerships Program of Australian Department of Climate Change and Energy Efficiency.

REFERENCES

Allan, R., and M. Haylock, 1993: Circulation features associated with the winter rainfall decrease in southwestern Australia. *J. Climate*, **6**, 1356–1367.

Ansell, T. J., C. J. C. Reason, I. N. Smith, and K. Keay, 2000: Evidence for decadal variability in southern Australian rainfall and relationships with regional pressure and sea surface temperature. *Int. J. Climatol.*, **20**, 1113–1129.

Bates, B. C., P. Hope, B. Ryan, I. Smith, and S. Charles, 2008: Key findings from the Indian Ocean climate initiative and their impact on policy development in Australia. *Climatic Change*, **89**, 339–354.

Cai, W. J., and I. G. Watterson, 2002: Modes of interannual variability of the Southern Hemisphere circulation simulated by the CSIRO climate model. *J. Climate*, **15**, 1159–1174.

Cai, W. J., G. Shi, and Y. Li, 2005: Multidecadal fluctuations of winter rainfall over southwest Western Australia simulated in the CSIRO Mark 3 coupled model. *Geophys. Res. Lett.*, **32**, L12701, doi: 10.1029/2005GL022712.

Cai, W. J., P. Van Rensch, S. Borlace, and T. Cowan, 2011: Does the Southern Annular Mode contribute to the persistence of the multidecade-long drought over southwest Western Australia? *Geophys. Res. Lett.*, **38**, L14712, doi: 10.1029/2011GL047943.

Chang, C. P., Y. S. Zhang, and T. Li, 2000: Interannual and interdecadal variations of the East Asian summer monsoon and tropical Pacific SSTs. Part I: Role of the subtropical ridge. *J. Climate*, **13**, 4310–4325.

Connolley, W. M., 2002: Long-term variation of the Antarctic Circumpolar Wave. *J. Geophys. Res.*, **108**, doi: 10.1029/2000JC000380.

Ding, Y. H., 1994: The summer monsoon in East Asia. *Monsoons over China*, Kluwer Academic, 1–9.

Ding, Y. H., and C. J. Chan, 2005: The East Asian summer monsoon: A review. *Meteor. Atmos. Phys.*, **89**, 117–142.

England, M. H., C. C. Ummenhofer, and A. Santoso, 2006: Interannual rainfall extremes over southwest Western Australia linked to Indian Ocean variability. *J. Climate*, **19**, 1948–1969.

Feng, J., J. P. Li, and Y. Li, 2010a: A monsoon-like southwest Australian circulation and its relation with rainfall in southwest Western Australia. *J. Climate*, **23**, 1334–1353.

Feng, J., J. P. Li, and Y. Li, 2010b: Is there a relationship between the SAM and southwest Western Australian winter rainfall? *J. Climate*, **23**, 6082–6089.

Feng, J., and J. P. Li, 2013: Contrasting impacts of two types of ENSO on the boreal spring Hadley circulation. *J. Climate*, **26**, 4773–4789.

Frederiksen, J. S., and C. S. Frederiksen, 2007: Interdecadal changes in Southern Hemisphere winter storm track modes. *Tellus*, **59**A, 599–617.

Gong, D. Y., and S. W. Wang, 1999: Definition of Antarctic Oscillation index. *Geophys. Res. Lett.*, **26**, 459–462.

Guo, Q. Y., J. N. Cai, X. M. Shao, and W. Y. Sha, 2003: Interdecadal variability of East–Asian summer monsoon and its impact on the climate of China. *Acta Geographica Sinica*, **58**, 569–576. (in Chinese)

Hendon, H. H., D. W. Thompson, and M. C. Wheeler, 2007: Australian rainfall and surface temperature variations associated with the Southern Hemisphere Annular Mode. *J. Climate*, **20**, 2452–2467.

Hope, P. K., 2006: Projected future changes in synoptic systems influencing southwest Western Australia. *Climate Dyn.*, **26**, 765–780.

Hu, Z. Z., 1997: Interdecadal variability of summer climate over East Asia and its association with 500 hPa height and global sea surface temperature. *J. Geophys. Res.*, **102**, 19 403–19 412.

Indian Ocean Climate Initiative (IOCI), 2002: Climate variability and change in southwest Western Australia. Indian Ocean Climate Initiative Panel, Perth, September 2002, 34 pp.

Jones, D. A., and G. Bead, 1998: Verification of Australian monthly district rainfall totals using high resolution gridded analyses. *Aust. Meteor. Mag.*, **47**, 41–54.

Kalnay, E., and Coauthors, 1996: The NCEP/NCAR 40–year reanalysis project. *Bull. Amer. Meteor. Soc.*, **77**, 437–471.

Lau, K. M., and M. T. Li, 1984: The monsoon over East Asia and its global association—A survey. *Bull. Amer. Meteor. Soc.*, **65**, 116–125.

Li, F., L. E. Chambers, and N. Nicholls, 2005: Relationships between rainfall in the southwest of Western Australia and near-global patterns of sea surface temperature and mean sea level pressure variability. *Aust. Meteor. Mag.*, **54**, 23–33.

Li, J. P., and Q. C. Zeng, 2002: A unified monsoon index. *Geophys. Res. Lett.*, **29**, 1274, doi: 10.1029/2001GL013874.

Li, J. P., J. Feng, and Y. Li, 2012: A possible cause of decreasing summer rainfall in northeast Australia. *Int. J. Climatol.*, **32**(7), 995–1005.

Lyons, T. J., 2002: Clouds prefer native vegetation. *Meteor. Atmos. Phys.*, **80**, 131–140.

Marshall, G. J., 2003: Trends in the Southern Annular Mode from observations and reanalyses. *J. Climate*, **16**, 4134–4143.

Meneghini, B., S. Ian, and I. N. Smith, 2007: Association between Australian rainfall and the Southern Annular Mode. *Int. J. Climatol.*, **27**, 109–121.

Nan, S. L., and J. P. Li, 2003: The relationship between summer precipitation in the Yangtze River valley and the boreal spring Southern Hemisphere Annular Mode. *Geophys. Res. Lett.*, **30**, 2266, doi: 10.1029/2003GL018381.

Nicholls, N., 1989: Sea surface temperatures and Australian winter rainfall. *J. Climate*, **2**, 965–973.

Pitman, A. J., G. T. Narisma, R. A. Pielke, and N. J. Holbrook, 2004: Impact of land cover change on the climate of southwest Western Australia. *J. Geophys. Res.*, **109**, D18019, doi: 10.1029/2003JD004347.

Ramage, C. S., 1978: *Monsoon Meteorology*. Science Press, 1–4.

Rayner, N. A., D. E. Parker, E. B. Horton, C. K. Folland, L.

V. Alexander, D. P. Rowell, E. C. Kent, and A. Kaplan, 2003: Global analyses of sea surface temperature, sea ice, and night marine air temperature since the late nineteenth century. *J. Geophys. Res.*, **108**(D14), 4407, doi: 10.1029/2002JD002670.

Smith, I. N., P. McIntosh, T. J. Ansell, C. J. C. Reason, and K. Mclnnes, 2000: Southwest Western Australian winter rainfall and its association with Indian Ocean climate variability. *Int. J. Climatol.*, **20**, 1913–1930.

Smith, T. M., and R. W. Reynolds, 2004: Improved extended reconstruction of SST (1854–1997). *J. Climate*, 17, 2466–2477.

Tao, S. Y., and S. Y. Xu, 1962: Circulation characteristics in association with persistent summer drought and flood in the Yangtze-Huaihe River reaches. *Acta Meteorologica Sinica*, **32**, 1–18. (in Chinese)

Tao, S. Y., and L. X. Chen, 1987: A review of recent research on the East Asian summer monsoon in China. *Monsoon Meteorology.* Vol. 7, *Oxford Monographs on Geology and Geophysics*, Oxford University Press, 60–92.

Telcik, N., and C. Pattiaratchi, 2014: Influence of northwest cloudbands on southwest Australian rainfall. *J. Climatol*., 2014, doi: 10.1155/2014/671394.

Thompson, D. W. J., and J. M. Wallace, 2000: Annular modes in the extratropical circulation. Part I: Month-to-month variability. *J. Climate*, **13**, 1000–1016.

Timbal, B., and J. M. Arblaster, 2006: Land cover change as an additional forcing to explain the rainfall decline in the southwest of Australia. *Geophys. Res. Lett.*, **33**, L07717, doi: 10.1029/2005GL025361.

Timbal, B., J. M. Arblaster, and S. Power, 2006: Attribution of the late-twentieth-century rainfall decline in southwest Australia. *J. Climate*, **19**, 2049–2062.

Visbeck, M., 2009: A station-based Southern Annular Mode index from 1884 to 2005. *J. Climate*, **22**, 940–950.

Wang, B., and Q. H. Ding, 2006: Changes in global monsoon precipitation over the past 56 years. *Geophys. Res. Lett.*, **33**, L06711, doi: 10.1029/2005GL025347.

White, W. B., 2000: Influence of the Antarctic circumpolar wave on Australian precipitation from 1958 to 1997. *J. Climate*, **13**, 2125–2141.

Zhu, Q. G., J. R. Lin, and S. W. Shou, 1992: *The Principles and Methods of Synoptic*. Meteorological Press, 150–164. (in Chinese)